THE EFFECT OF PROTONATION AND ELECTRICAL INTERACTIONS ON THE STEREOCHEMISTRY OF RETINAL SCHIFF BASES

PAUL TAVAN,* KLAUS SCHULTEN,* AND DIETER OESTERHELT‡
*Physik Department, Technische Universität München, 8046 Garching, Federal Republic of Germany;
and ‡Max-Planck-Institut für Biochemie, 8033 Martinsried, Federal Republic of Germany

ABSTRACT   Based on quantumchemical MNDOC calculations it is shown that the ground-state properties of a retinal Schiff base depend sensitively on its protonation state and charge environment. This is exemplified for the equilibrium geometry, for the distribution of partial charges and, in particular, for the thermal isomerization barriers around the π-bonds. It is demonstrated that a protein, by protonating the retinal Schiff base and by providing one or two negative ions in its environment, can reduce double-bond isomerization barriers from 50 kcal/mol for the unprotonated compound to ~ 5 kcal/mol and can increase single bond barriers from 5 kcal/mol to ~ 20 kcal/mol. Thereby, the specific location of the ions relative to the polyene chain of the protonated retinal Schiff base determines the barrier heights. The results explain the ground-state isomerization reactions of retinal observed in bacteriorhodopsin and in squid retinochrome.

INTRODUCTION

Bacteriorhodopsin (BR) in the purple membrane of *Halobacterium halobium* acts as a light-driven proton pump (1, 2). Retinal forms the chromophore of BR (see Fig. 1), is bound as a protonated Schiff base to the lysine residue 216, and in the light-adapted state absorbs at 568 nm. Upon light excitation BR enters a reaction cycle in which at least five ground state intermediates of the chromophore have been identified spectroscopically. Only the primary reaction step is of photochemical nature. This step proceeds within < 10 ps and entails an all-*trans* → 13-*cis* isomerization of retinal. The resulting red-shifted photoproduct K_{590} stores 16 kcal/mol of the absorbed light energy (3). K_{590} may actually not be the primary photoproduct but rather may be preceded by yet earlier discernible intermediates. In subsequent thermally activated reactions, for which rate constants ranging from 10^6 to 10^2 s^{-1} have been measured, this energy is used to translocate at least one proton across the membrane and to drive BR back to its original conformation. In this dark phase of the cycle, which is accompanied by protein conformational changes, a transient deprotonation of the Schiff base occurs and retinal reisomerizes within milliseconds to the all-*trans* geometry. Thermal isomerizations of retinal have been observed also in squid retinochrome (11-*cis* → 13-*cis* → all-*trans*) (4) and during dark adaptation of initially light-adapted BR_{568} (all-*trans* → 13, 15-di-*cis*) (5, 6, 7).

Retinal belongs to the family of polyene dyes, which are well known for their characteristic structure of alternating single and double π-electron bonds. In the ground state a rotation around double bonds is prevented by very high barriers of activation, typically of ~ 50 kcal/mol. Single bonds, in contrast, exhibit only low barriers of ~ 5 kcal/mol (8, 9). Single-bond rotations proceed readily within less than a nanosecond whereas thermal double-bond isomerizations are essentially unobservable. A strong perturbation of the polyene bond pattern is, therefore, a prerequisite for retinal to isomerize in the ground state around a double bond, as observed in the dark phase of the BR reaction cycle on a millisecond time scale, and in squid retinochrome and during dark adaptation of BR_{568} on a time scale of minutes. In BR such a perturbation is induced by the protonation of the Schiff-base nitrogen of the chromophore (10). The effect of the protonation is witnessed by the strong bathochromic shift of the absorption maximum from ~ 360 nm for the unprotonated Schiff base (11) to values ranging between 430 nm (12) and 610 nm (13) for the protonated chromophore inside the protein. This shift can be explained by arguing that the positive charge of the added proton attracts a π-system towards the terminal nitrogen, thereby transforming retinal to a polyenylic cation (11, 14). Such cations exhibit, in fact, absorption bands strongly red-shifted with respect to those of the parent polyenes, e.g., a red shift of more than 200 nm for a polyene isoelectronic with the conjugated π-system of retinal (14, 15, 16).

However, the transformation of retinal into a polyenylic ion does not only result in a lowering of the optically allowed excited state but also alters the ground-state bond structure. This has been shown in reference 17 on the basis of quantumchemical MINDO/3 calculations involving
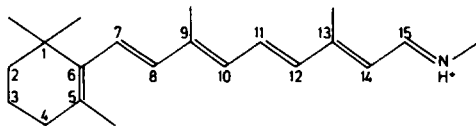
FIGURE 1 The Schiff base of retinal is shown. The chromophore is attached through the terminal nitrogen to a lysine residue of bacteriorhodopsin.

only a fragment of retinal. Because all steps in the BR pump cycle after the primary photophysical event involve ground state reactions only, we want to address ourselves in this paper to the ground-state stereochemical properties of the BR chromophore. Using as a quantumchemical tool the recently developed MNDOC method (18), we will show how a protein like bacterio-opsin, by protonating the terminal nitrogen and by providing an appropriate charge environment, can steer the stereochemical properties of retinal. In the section entitled Models for the Protein-Chromophore Interaction in BR, we will first discuss the available evidence concerning the interaction between retinal and its protein environment in BR and develop some of the model concepts on which our study is based. The following section introduces the quantumchemical methods. The section entitled Equilibrium Structures of Retinal Schiff Bases presents the calculated equilibrium structure of a retinal Schiff base in the protonated and unprotonated state. This investigation is extended in the section entitled Effect of Protonation on Isomerization Barriers to the ground-state activation energies for thermal isomerization around the single and double bonds of retinals conjugated π-system. This section contains the key result of the paper that is the demonstration that protonation partially reverses the single and double bond character of a retinal Schiff base. The section entitled Influence of Anions on the 13–14 Isomerization Barrier demonstrates how these effects are influenced by negatively charged groups at the chromophore site. As a measure for the perturbation of the retinal bond structure, we calculate the relevant barriers for isomerization. Earlier π-electron calculations (19, 20) have indicated already that these barriers should be strongly influenced by negative charges. In the section entitled Charge Separation Contribution to Isomerization Barriers, we show to what extent the thermal activation energies can be altered in a protein environment if bond rotations are accompanied by a charge separation between a negative counterion and the Schiff-base proton and if the protein dielectric properties are taken into account. A short summary concludes the paper.

MODELS FOR THE PROTEIN-CHROMOPHORE INTERACTION IN BR

Detailed information about the structure of the binding site of retinal in BR_{568} and about its conformational changes during the the photoreaction cycle is still lacking.

Any attempt to model the interaction between the protein and retinal in the purple membrane relies, therefore, on some speculations relating the available data.

It is known that the retinal Schiff base (RSB) is protonated during nearly all stages of the cycle, with the exception of the intermediate M_{410} (1, 2). Because the absorption maximum of the chromophore changes greatly during the pump cycle and upon variation of certain external conditions like pH or salt concentration, the interaction between the protein and retinal must change correspondingly. The size of the spectral red shift of the absorption maximum of the protonated retinal Schiff base ($RSBH^+$) is determined mainly by the interaction of the positive charge at the nitrogen with the polyene π-system (21, 22, 23). If one accepts that the transformation into a retinylic cation is completed and the spectral red shift enhanced by removing a possible counterion from the proton at the terminal nitrogen or by placing additional negative charges along the polyene backbone near the cyclohexene ring (24), one is led to several conclusions concerning the RSB environment in BR. First, one can conclude from titration experiments (25) and from a study (26) of the changes in the protonation state of BR during reconstitution of the chromophore that there exists a counterion of pK 3 in the vicinity of the proton at the Schiff base nitrogen (27). A neutralization of this counterion by protonation can explain the bathochromic shift to 605 nm observed at low pH, since such a neutralization renders the transformation of the $RSBH^+$ into a retinylic cation complete. Similar arguments apply to the red-shifted K and O intermediates of the reaction cycle absorbing at 590 and 640 nm, respectively. Both species appear as immediate products of isomerization reactions involving a rotation around the 13–14 bond of the $RSBH^+$. In the case of K the isomerization is certain, because this primary photoproduct of all-trans BR_{568} contains a distorted 13-cis $RSBH^+$ (28, 29). In the case of O an isomerization is likely since the $RSBH^+$ is all-trans in this intermediate (30) and is 13-cis in the unprotonated precursor M_{410}. In both cases the bond rotation may separate the Schiff-base proton and its respective counterion which can explain the strong red-shift.

The above statements about the possible existence of a counterion close to the terminal nitrogen in BR are confirmed by recent pH-jump experiments that yielded above pH 11.5 a strongly blue-shifted BR species absorbing at 460 nm. This species contains an unprotonated RSB chromophore as was shown by resonance Raman spectroscopy (31). From these measurements a pK value of 13.3 has been derived for the RSB in BR. This pK value, which is very large compared to solution values of ~6.5, points towards the stabilizing effect of an anion in the vicinity of the protonated nitrogen. However, as we will argue below, a stabilization of the Schiff-base proton can also be induced by a negative charge that is situated towards the cyclohexene ring and interacts with the π-system. The latter

explanation would also rationalize the spectral maximum at 460 nm, which is very much in the red range for an unprotonated RSB. A negative charge somewhere over the π-electron backbone of retinal could produce, however, such a spectral shift. This explanation of the spectral shift is also in accordance with earlier BR reconstitution experiments that revealed the existence of a 430–460 nm intermediate prior to the establishment of the Schiff-base linkage (32, 33). It was shown that the formation of this intermediate depends on at least one group with a pK of 3.8, and that another group with a pK of 4.5 as well as a base with a $pK > 10.5$ are necessary prerequisites for the completion of the reaction (34, 35). One may speculate that the latter group is the ϵ-amino group of the lysine residue to which retinal becomes covalently bound. According to reference 26 the group with the pK value of 4.5 has to be identified with the counterion, because its pK is shifted to a value of 3.0 upon interaction with the protonated Schiff base. In these measurements a pK shift from 7 to 9 of yet another group had been observed. We conclude, therefore, that in addition to the counterion at the nitrogen there exist in the immediate environment of the polyene moiety of the RSB in BR at least one additional negatively charged group (pK 3.8) and a couple of polar groups.

Chromophore reconstitution experiments with retinal analogues containing shortened chains of conjugated double bonds yielded shifts of the visible absorption maximum that fit a model with one anion 3.0 Å distant from the Schiff base and another 3.5 Å from the C_5 atom of the cyclohexene ring (36). Recently, additional material has been presented by the same authors to support their model using the same type of arguments. Spectral shifts of cyanine dyes upon reconstitution with bacterio-opsin (37) did compare well with the results of PPP-CI calculations (38, 39). However, since such calculations cannot unequivocally determine the positions of the anions, we still consider the details of the charge distribution in the retinal binding site of BR to be unknown, although we think that the "two external point charge model" is quite plausible.

Considerations like those sketched above led us to a three-step approach for our quantumchemical investigation of the ground state stereochemical properties of retinal induced by bacterio-opsin. In a first step we will study the effect of pure protonation on a RSB using the corresponding cation as a model. Then we will introduce a counterion and vary its distance from the proton at the Schiff-base nitrogen. Finally we will add a second anion and move it at a distance of 3 Å along the polyene backbone, keeping the position of the first anion fixed. For the sake of simplicity we will use the results on the cation as a reference for comparisons with experimental data on the BR chromophore. It will become apparent from the investigation of the effects of negative charges in a protein dielectric environment on the stereochemical properties of a RSBH$^+$ that this simplification does not impose severe restrictions

on our conclusions (see the sections entitled Influence of Anions on the 13–14 Isomerization Barrier, and Charge Separation Contribution to Isomerization Barriers).

QUANTUMCHEMICAL METHODS

We have carried out MNDOC calculations (18) for the heat of formation and for isomerization potential surfaces of protonated and unprotonated retinal Schiff bases and related model compounds. MNDOC is an improved version of MNDO (modified neglect of diatomic overlap) (40) allowing the explicit inclusion of electron correlation effects. This method furnishes the most reliable semiempirical description of ground-state properties of organic molecules containing the elements H, C, N and O. We have extended the method to include fluorine (F) because we wanted to include this atom in our calculations as a model anion (Tavan, P., and K. Schulten, unpublished results). Electron correlation is treated in MNDOC by second-order perturbation theory using Brillouin-Wigner expansions combined with Epstein-Nesbet energy denominators (BWEN) (41, 42).

As retinal contains more than 150 electrons, routine ab initio calculations for many points on a reaction path would not have been feasible computationally. Even for a semiempirical all-valence electron method like MNDOC, the number of electrons is very large. Therefore, we had to restrict the geometry optimization to the SCF level. However, this treatment represents a reasonable approximation to the correlated MNDOC procedure (18). For the determination of the equilibrium geometries, nearly all geometric variables were relaxed except for the torsional angles in the region between C_7 and the terminal nitrogen of the polyene chain for which a strictly planar conformation was assumed. For the calculation of isomerization potential curves only a subset of relevant geometric degrees of freedom was optimized. This subset comprised $\sim$ 30 variables and included the C—C and C—H bond lengths and angles along the retinal polyene chain as well as the torsional angles of the CH_3-groups in the vicinity of the respective reaction coordinate. For instance, in the calculations of the potential curves for the torsion around the 13–14 double bond (see the sections entitled Effect of Protonation on Isomerization Barriers, Influence of Anions on the 13–14 Isomerization Barrier, and Charge Separation Contribution to Isomerization Barriers), in addition to the polyene geometry parameters all degrees of freedom of the methyl group at C_{13} were optimized because in the course of the rotation this group interacts sterically with the hydrogen at C_{15}. At each point on the reaction path the SCF geometry optimization was followed by a calculation of the BWEN correlation correction to the Hartree-Fock energy. The extended computations necessary were carried out on a CRAY-1, by employing a program code optimized to the parallel processing facilities of this installation.

Although MNDOC is superior in many respects (accuracy of calculated bond lengths, bond angles, heat of

formation, etc.) to earlier semiempirical methods like CNDO (43), MINDO/3 (44) or MNDO (40), it shares a common drawback (45, 46). All these methods systematically underestimate the torsional stability of C—C single bonds. For example, in the case of the central single bond of butadiene, MNDO predicts an isomerization barrier of only 0.5 kcal/mol, and the MNDOC barrier is 1.1 kcal/mol, whereas the experimental value is 5 kcal/mol (8). If sterical interactions compete with the torsional stability of π-single bonds this failure can lead to the prediction of strongly twisted polyene geometries. However, if one fixes such torsional angles during the geometry optimization e.g., to the experimental values, then MNDOC yields qualitatively correct descriptions of equilibrium geometries even for molecules as large as retinal (see Equilibrium Structures of Retinal Schiff Bases).

The MNDOC Method allows an increase of the torsional stability of C—C single bonds by a change of the bond-length dependence of the π-π resonance integral (Tavan, P., and K. Schulten, unpublished results). With a correspondingly reparametrized method, termed MNDOC/T, we obtained for butadiene a single bond isomerization barrier of 1.6 kcal/mol, i.e., the torsional stability has been improved but is still too small. Consequently, the MNDOC/T results quoted below may serve only as an estimate for the necesary corrections to the MNDOC torsional barriers of those C—C π-bonds, which are $\gtrsim 1.4$ Å.

EQUILIBRIUM STRUCTURES OF RETINAL SCHIFF BASES

Fig. 3 shows the bond lengths and bond angles of the carbon skeleton of the unprotonated RSB shown in Fig. 2 that were obtained by a MNDOC-SCF geometry optimization. Our calculations have demonstrated (Tavan, P., and K. Schulten, unpublished results) that the replacement of the terminal NCH_3 residue by an oxygen atom affects
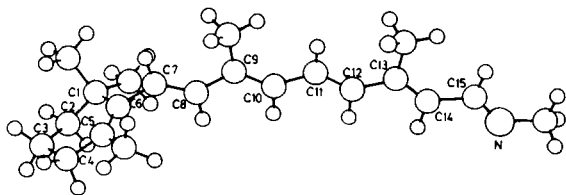

FIGURE 2 The geometry of the unprotonated retinal Schiff base drawn to scale as predicted by the MNDOC method is shown. Throughout this paper we use the following nomenclature for the various retinal derivatives: We characterize them by the residue X appending at the polyene chain at C_{15} and by the structure Y of the compound up to X. If Y matches retinal we designate it as RETINAL. For many calculations we replaced the carbon atoms C_1 and C_4 by hydrogen atoms, i.e., we omitted most of the cyclohexene ring keeping, however, the MNDOC geometry of RETINAL in the region between C_5 and C_8. For these smaller compounds Y is named RET (see Fig. 7). If, in a calculation, ring and chain are forced to be coplanar a prefix PL- is added to Y. With these conventions the compound in this figure is RETINAL-NCH₃.
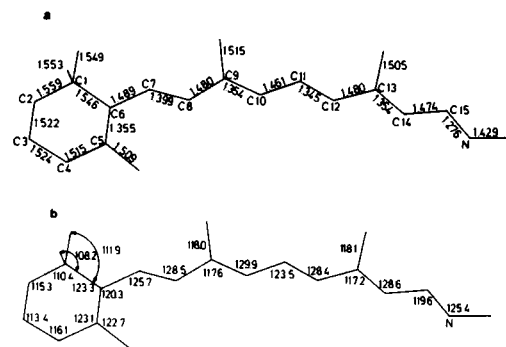

FIGURE 3 The calculated bond lengths and bond angles of the carbon skeleton of RETINAL-NCH₃ are shown; for the purpose of this drawing, the dihedral angle between the cyclohexene ring and the polyene chain of 83° has been set to 0°; (a) bond lengths, (b) bond angles.

the retinal geometry only slightly. Consequently, the crystal-structure data for retinal (47) shown in Fig. 4 can be taken as an experimental reference for the theoretical results in Fig. 3. We find comparing these data that MNDOC reproduces the crystal geometry quite well, the deviations being a few hundredths of an angstrom for the bond lengths and 3° for the bond angles at most. The typical banana-type curvature of the polyene chain is somewhat exaggerated by the MNDOC method as it predicts the bond angles adjacent to the methyl groups to be 128.8° on the average whereas a value of 126.3° is observed. The conformation of the cyclohexene ring can be characterized by the C_2—C_1—C_6—C_5 torsion angle. This angle measures 19° in the retinal crystal and is predicted to be 21° by MNDOC. However, this good agreement may be accidental because the crystallographic bond angles and, in particular, torsion angles depend sensitively on the details of the crystal structure (48). The only serious deviation of our quantumchemical description from the experimental findings is the dihedral angle between the plane of the ring and that of the chain. Our calculations consistently predict a torsional angle of 83°, which is larger than the observed
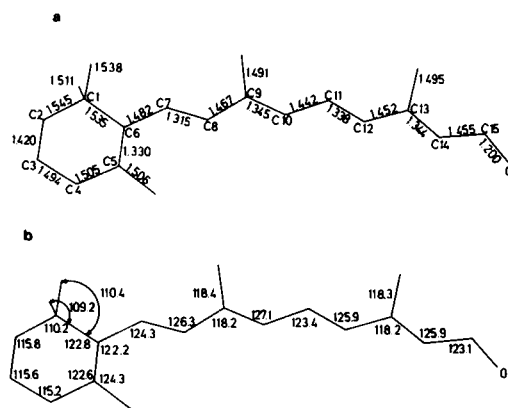

FIGURE 4 Retinal crystal structure data from reference 45 is shown; (a) bond lengths, (b) bond angles.

angle of 62°, because MNDOC does not assign enough torsional stability to the 6–7 π-single bond to compete with the steric interaction between the methyl groups at C_1 and C_5 and the hydrogens at C_7 and C_8.

Protonation of a RSB induces a drastic change of its equilibrium geometry as shown in Fig. 5. Although bond and torsion angles are nearly unaffected, the pattern of alternating short and long bonds exhibited clearly by RETINAL-NCH$_3$ (see the caption to Fig. 2 for the nomenclature) is partially destroyed in RETINAL-NH$^+$CH$_3$, in which the short π-bonds have become longer and the long bonds have become shorter (see Figs. 3 and 5). This tendency is more pronounced towards the terminal nitrogen, so that the 13–14 double bond is even longer than the neighboring 14–15 single bond. This observation suggests that protonation of a RSB exercises a selective influence on the π-bonds, and should affect in particular the stereochemical properties of the terminal region of the polyene chain.

The weakening of the double bonds and the strengthening of the single bonds is caused by a partial migration of a π-electron charge to the terminal nitrogen, rendering the π-system positive. This is illustrated in Fig. 6, which compares the partial charges of the unprotonated and the protonated Schiff base RETINAL—NCH$_3$ and RETINAL—NH$^+$CH$_3$, respectively. The charge shift is seen to be effected through the induction of strong local dipoles between the odd and even numbered carbons in the π-system (49, 50). One observes that more electron density is subtracted from the odd numbered carbon atoms than is added to the even numbered ones; the missing charge is shifted to the terminal nitrogen. With the progressive elongation of the double bonds the strength of the asymmetric dipoles increases along the chain. Consequently, the electron density loss is largest at C_{13} and the corresponding gain is most pronounced at C_{14}.

All protonation effects are confined essentially to the polyene moiety of the RSBH$^+$. Fig. 7 presents the MNDOC charge distribution for the protonated model compound RET—NH$^+$CH$_3$, which comprises the polyene
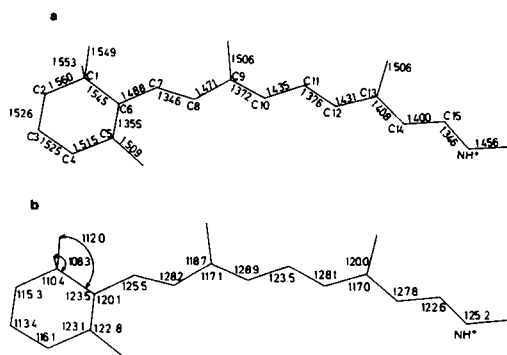
part of RETINAL—NH$^+$CH$_3$ only. A comparison with the data in Fig. 6 b shows that along the polyene chain between C_7 and the terminal nitrogen the partial charges of the two cations are virtually identical. Corresponding statements hold for the bond lengths and angles. Consequently, the influence of the cyclohexene ring on the structure of the chain is weak and the RET—NCH$_3$ and RET—NH$^+$CH$_3$ molecules should be excellent models for the study of stereochemical protonation effects in that part of the chain which ranges from C_9 to N. Similar investigations have shown that the perturbation of the chain structure caused by the methyl group attached to the nitrogen is also very small, such that the RET—NH and RET—NH$_2^+$ molecules are suitable models as well as long as steric hindrances induced by the terminal methyl group upon bond isomerization can be neglected. In order to reduce the computational effort we have applied, therefore, most calculations to these smaller model compounds.

EFFECT OF PROTONATION ON ISOMERIZATION BARRIERS

The change of the polyene structure caused by the protonation of the Schiff base is most clearly and dramatically reflected by the ground-state isomerization barriers. The

Figure 5 Calculated equilibrium geometry of the protonated Schiff base RETINAL-NH$^+$CH$_3$ (see captions to Figs. 2 and 3).
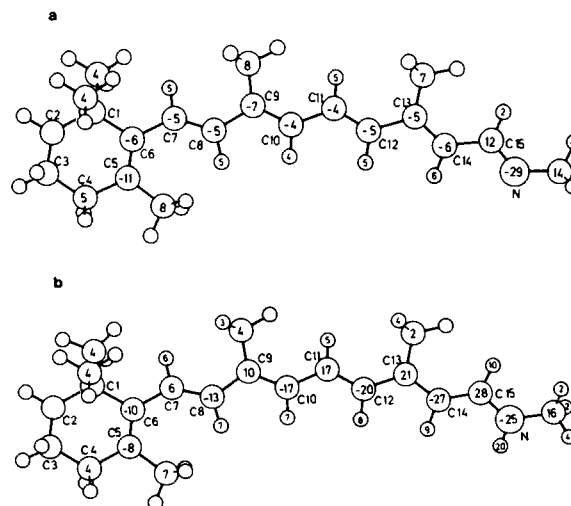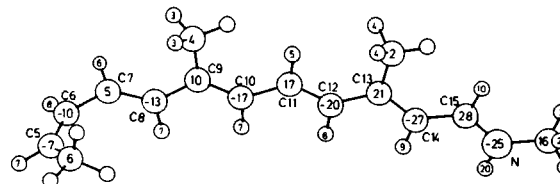

Figure 7 Partial charges of the protonated model compound RET-NH$^+$CH$_3$ (see captions to Figs. 2 and 6 for further information).

TABLE I
ISOMERIZATION BARRIERS OF UNPROTONATED RET – NH

	MNDOC			
	SCF		BWEN	
R_i	E_a^*	$E_{(t-c)}\ddagger$	E_a^*	$E_{(t-c)}\ddagger$
R_{13}	56.1	−0.1	46.8	0.2
R_{14}	−0.5	−1.0	−1.9	−1.0
	MNDOC/T			
R_{14}	0.7	0.0	1.4	0.0

MNDOC and MNDOC/T torsional barriers E_a^* and relative energies of cis and trans isomers $E_{(t-c)}\ddagger$ for the rotations R_i, i = 14, 15, around the $i - i + 1$ bonds of the unprotonated model RSB RET-NH. Energies are given in kilocalories per mole.
*The energy E_a of the conformation twisted by 90° is defined relative to the lower of the two isomers.
‡E (trans) − E (cis).

MNDOC-SCF and MNDOC-BWEN results for the thermal activation energies E_a for rotation around various bonds along the polyene chain are collected in Tables I and II for the unprotonated and protonated model RSB's RET—NH and RET—NH$_2^+$, respectively.

For the unprotonated compound only the two torsional barriers around the 13–14 and 14–15 π-bonds have been

TABLE II
ISOMERIZATION BARRIERS OF PROTONATED RET-X

		MNDOC			
		SCF		BWEN	
−X	R_i	E_a^*	$E_{(t-c)}\ddagger$	E_a^*	$E_{(t-c)}\ddagger$
−NH$_2^+$	R_9	24.8	0.1	25.6	1.5
	R_{11}	18.3	−4.0	19.1	−3.7
	R_{12}	5.8	0.1	7.6	0.5
	R_{13}	11.2	0.5	11.5	1.0
	R_{14}	13.1	−4.2	13.0	−3.0
−NH$^+$CH$_3$	R_{15}	16.3	−1.2	17.2	−1.5
−NH$_2^+$	$R_{11} + R_{13}$	18.8	−3.5	19.7	−3.8
−NH$^+$CH$_3$	$R_{13} + R_{15}$	17.6	−0.8	19.5	−0.5
−NH$_2^+$	$R_{13} + R_{14}$	37.7	−3.9	35.2	−3.7
		MNDOC/T			
−NH$_2^+$	R_{13}	11.2	0.5	12.7	0.4
	R_{14}	18.9	−3.3	20.4	−3.1

MNDOC and MNDOC/T torsional barriers E_a^* and relative energies of cis and trans isomers $E_{(t-c)}\ddagger$ for the rotations R_i, i = 9, . . . , 15, around the $i - i + 1$ bonds and for the simultaneous rotations $R_i + R_j$ around the $i - i + 1$ and $j - j + 1$ bonds of the protonated model retinal Schiff base RET − X. X is the residue appending at the carbon atom C_{15} of the polyene moiety. Energies are given in kilocalories per mole.
*The energy E_a of the conformation twisted by 90° is defined relative to the lower of the two isomers.
‡E (trans) − E (cis).

calculated to represent the behavior of typical polyene double and single bonds. The MNDOC-BWEN result of 46.8 kcal/mol for the rotation R_{13} (rotation around the 13–14 bond, see the caption to Table I for the nomenclature) is well within the expected order of magnitude and testifies the extraordinary stability of double bonds with respect to thermal isomerization reactions. In contrast, the 14–15 single bond is found to be unstable against torsional motions. The prediction of a shallow potential minimum ($E_a = -1.9$ kcal/mol) at the conformation twisted by 90° around the 14–15 bond is due to the fact that MNDOC overestimates the weak steric interaction between the methyl group at C_{13} and the hydrogen atom at C_{15} and underestimates the considerable torsional stability of the 14–15 π-single bond. This failure is qualitatively corrected by MNDOC/T in that this method assigns a positive activation energy of 1.4 kcal/mol to R_{14}. The correct value should be < 5 kcal/mol.

Protonation reduces the C—C double-bond isomerization barriers progressively along the chain. The predicted barriers are 25.6 kcal/mol for R_9, 19.1 kcal/mol for R_{11}, and 11.5 kcal/mol for R_{13}. The latter barrier allows a thermal isomerization reaction around the 13–14 bond to proceed within milliseconds. Our calculation rationalizes the observation that such thermal isomerization occurs in BR in connection with the formation of the O intermediate. Conversely, MNDOC-BWEN predicts a considerable increase of torsional stability for the single bonds. The predicted isomerization barriers in this case are 7.6 kcal/mol for R_{12} and 13.0 kcal/mol for R_{14}. The surprising result emerges that the ground state activation energy for the single bond isomerization all-trans → 14s-cis is larger than the activation energy for the double-bond isomerization all-trans → 13-cis. If one employs the MNDOC/T method this reversal of bond stability is even more pronounced: the calculated activation energies are 12.7 kcal/mol for R_{13} and 20.4 kcal/mol for R_{14}. On the time scale of the BR reaction cycle an activation energy like the latter would prevent a 14s-cis ↔ 14s-trans isomerization. Fig. 8 a for R_{13} and Fig. 8 b for R_{14} illustrate the protonation effects discussed above showing typical torsional potential curves as obtained from MNDOC-BWEN and MNDOC/T-SCF calculations on the model compounds RET—NH and RET—NH$_2^+$.

Our MNDOC-BWEN double-bond isomerization barriers for the RSBH$^+$ are predicted at much lower values than those calculated in previous quantumchemical studies (17, 50). So, for instance, our R_{11} value of 19.1 kcal/mol is 9 kcal/mol lower than that predicted in reference 50 on the basis of an INDO-CISD treatment. In this case the difference is mainly due to the fact that in our calculation all essential geometric parameters were allowed to relax at each value of the torsional reaction coordinate, whereas in the calculation of reference 50 a polyene-type model geometry had been assumed for the RSBH$^+$ and had been kept fixed along the reaction path.
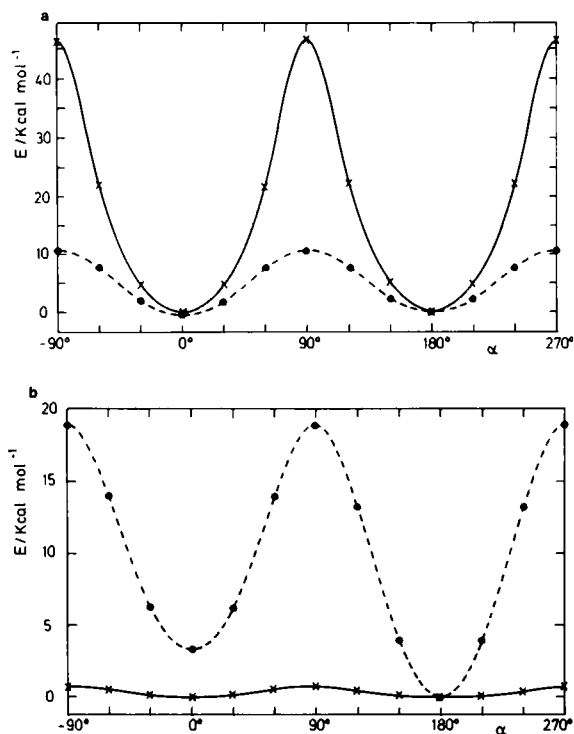
420

FIGURE 8 Effect of protonation on double-bond and single-bond isomerization potential curves for a model retinal Schiff base; (———) unprotonated compound; (---) protonated compound; the curves represent a cubic spline interpolation of the numerical values calculated at 30° intervals; all-*trans* is at a torsion angle α of 180°, the *cis* states are at 0°; (a) MNDOC-BWEN potential curves for R_{13}; (b) MNDOC/T-SCF potential curves for R_{14}.

The dependence of the torsional barriers on the protonation state entails the possibility of stereochemical *pK* shifts of a RSB. If, for instance, in the initial intermediates K and L of the BR reaction cycle the protein forces retinal into a strained conformation twisted around the 14–15 single bond, then, according to our data, the Schiff base can be converted into a strong acid, although it is a strong base with a *pK* value of 13.3 in the relaxed all-*trans* conformation of BR_{568}. As shown in Fig. 8 *b* an R_{14} torsion by 60° energetically shifts the protonated state by $\sim$ 14 kcal/mol relative to the unprotonated state. This shift corresponds to a reduction of the *pK* value by $\sim$ 10 units. Conversely, a torsion around a double bond can increase the *pK* value of the terminal nitrogen (51).

To test the validity of the conjecture that the smaller compounds RET—X provide an essentially correct description of the isomerization properties of the polyene moiety of a complete RSB we have calculated the 13–14 rotation potential curve for RETINAL—NH_2^+. The SCF result of 10.8 kcal/mol for the barrier height (see Table III) is in excellent agreement with the corresponding RET—NH_2^+ value of 11.2 kcal/mol. Inclusion of electron correlation by means of a BWEN treatment reduces the RETINAL—NH_2^+ barrier to 9.9 kcal/mol instead of yielding a small increase to 11.5 kcal/mol as in the case of

TABLE III
13–14 ISOMERIZATION BARRIER OF PROTONATED RETINAL

Compound	SCF		BWEN	
	$E_a{}^*$	$E_{(t-c)}\ddagger$	$E_a{}^*$	$E_{(t-c)}\ddagger$
RETINAL – NH_2^+	10.8	0.6	9.9	0.0
PL-RETINAL – NH^+CH_3	9.0	0.5	9.0	1.6

MNDOC torsional barriers $E_a{}^*$ and relative energies of *cis* and *trans* isomers $E_{(t-c)}\ddagger$ for the rotation R_{13} around the 13–14 bond of protonated RETINALs. Energies are given in kilocalories per mole.
*The energy E_a of the conformation twisted by 90° is defined relative to the lower of the two isomers.
$\ddagger E$ (*trans*) $- E$ (*cis*).

RET—NH_2^+. Because the resulting difference of 1.6 kcal/mol does not point toward any qualitatively different behavior of the two compounds and because, on the contrary, the lower RETINAL—NH_2^+ value even underlines the conclusions drawn from the discussion of the RET data, the restriction to the smaller compounds seems to be justified entirely.

Spectral investigations of BR reconstitution reactions yielded indications that bacterio-opsin may force retinal into a conformation in which ring and chain are coplanar (34, 35). We therefore calculated the R_{13} potential curve also for the planarized compound PL-RETINAL—NH^+CH_3. The effective enlargement of the π-system caused by the planarization yields a further reduction of the activation energy to 9.0 kcal/mol underlining, again, our inferences. In the section entitled Influence of Anions on the 13–14 Isomerization Barrier we will show that the protein can induce such a planarization by pure electrostatic interactions.

The small decrease of the R_{13} barrier height for the two protonated RETINAL molecules as compared to the RET—NH_2^+ model compound is due to the greater flexibility of their electron system in the region of the cyclohexene ring. The ring region affects the barriers because in the transition state for the rotation R_{13}, an additional and considerable shift of positive charge occurs towards this region. This is shown in Table IV, which presents the shifts DQ_i ($i = 9, \ldots, 15$) of the partial charges at the chain atoms C_7–C_{15} and N of RET—NH_2^+ in the 90° transition states of the bond rotations R_i. The charge shifts DQ_i are defined relative to the all-*trans* state, the charge distribution of which is also presented in Table IV. The location of the $i - i + 1$ π-bond broken in the 90° conformation is indicated by a line in the table. This line divides the polyene π-system into an initial part and a terminal part, the latter comprising the protonated Schiff base.

For all double-bond rotations ($i = 9, 11, 13, 15$) the transition state is characterized by an additional migration of electron charge density towards the terminal nitrogen of the $RSBH^+$. The charge shift of $\sim 25 \times 10^{-2}$ e increases the charge density at the nitrogen and decreases the

TABLE IV
TORSION INDUCED PARTIAL CHARGE SHIFTS FOR RET – NH_2^+

Atom	Q	DQ_9	DQ_{11}	DQ_{13}	DQ_{15}
C_7	+5	+24	+15	+8	+7
C_8	-13	-10	-7	-5	-4
C_9	+10	+27	+17	+11	+8
C_{10}	-17	-13	-5	-4	-3
C_{11}	+18	-5	+11	+7	+6
C_{12}	-21	+3	-7	+1	0
C_{13}	+21	-12	-12	+2	-2
C_{14}	-27	+3	+2	-4	+12
C_{15}	+28	-11	-10	-10	-2
N	-23	-8	-8	-10	-19

Atom	Q	DQ_{12}	DQ_{14}	DQ_{13+15}	DQ_{13+14}
C_7	+5	-5	-5	+11	+2
C_8	-13	+3	+3	-5	-1
C_9	+10	-8	-7	+12	+3
C_{10}	-17	+5	+4	-4	-1
C_{11}	+18	-11	-7	+6	+2
C_{12}	-21	0	+4	+2	+1
C_{13}	+21	+2	-9	+3	+3
C_{14}	-27	+2	-4	+8	-9
C_{15}	+28	+4	+10	-12	+4
N	-23	+6	+10	-19	+1

Shift DQ_i of the partial charges $Q(90°, i)$ at the C-atoms 7 – 15 and at the terminal nitrogen of RET – NH_2^+ upon rotation of the $i - i + 1$ bond by 90°; the partial charges Q of all-*trans* RET – NH_2^+ are also given; DQ_i is defined by $DQ_i = Q(90°, i) - Q$ (see text and caption to Figure 6 for further information). Also given are the charge shifts DQ_{13+15} and DQ_{13+14} for the rotations $R_{13} + R_{15}$ and $R_{13} + R_{14}$.

induced dipoles in the terminal part such that this region appears more like a polyene with alternating double and single bonds in an order opposite to that of the unprotonated retinal Schiff base. This behavior is proven by monitoring the change of the C—C bond lengths along the chain as a function of the torsion angle α, the reaction coordinate for R_i. As a typical example Fig. 9 shows the variation of the 10–11 single-bond length during the rotation R_9. The bond length is found to range between 1.435 Å in the all-*trans* and 9-*cis* conformations and 1.347
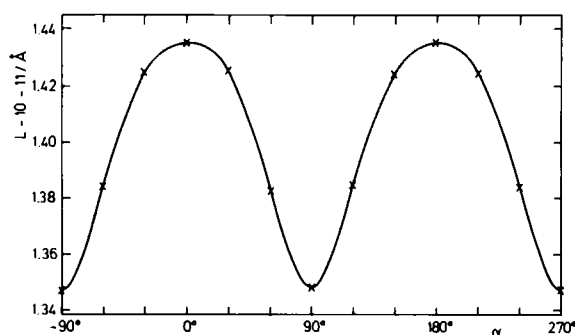

FIGURE 9 Relaxation of the 10–11 single-bond length in the course of the 9–10 double-bond isomerization for RET-NH_2^+; 9-*cis* is at $\alpha = 0°$.

Å in the transition state; this latter value corresponds to a strong π-double bond. Conversely, all former double bonds of the terminal part, i.e., 11–12, 13–14, 15–16, are strongly elongated upon double-bond rotations. From this analysis one can deduce bonding patterns for the transition states like the one drawn for R_9 in Fig. 10 *b*. (For comparison the bond pattern of all-*trans* RET—NH_2^+ has been given in Fig. 10 *a*.) The withdrawal of electron density from the initial region of the chain increases the induced dipoles (see Table IV) and, correspondingly, yields transition state bond lengths of an intermediate size of ~ 1.41 Å for all bonds in this region.

All the above statements have to be reversed if thermal single-bond isomerizations of a $RSBH^+$ are considered. As one can see from the charge shifts DQ_{12} and DQ_{14} in Table IV the transition states of single-bond isomerizations are characterized by a shift of electron density towards the initial part and a decrease of the induced dipoles in this region yielding, for example, in the case of R_{12} the schematic bond pattern shown in Fig. 10 *c*.

The bond patterns in Fig. 10 suggest that simultaneous rotations around two double bonds or two single bonds may have activation energies only slightly larger than isomerizations comprising one of these bonds only. Such bicycle-pedal-type rotations (52) could be preferred in a protein environment due to steric requirements. On the other hand, the patterns in Fig. 10 suggest that simultaneous isomerizations around a single and a double bond should have very high barriers of activation since torsion around a double bond strengthens the remaining single bonds and vice versa.

These hypotheses are confirmed by the examples for combined rotations $R_i + R_j$ in Table II. The barrier for the $R_{13} + R_{15}$ rotation around the 13–14 and 15–16 bonds is predicted by the MNOC-BWEN method at 19.5 kcal/mol, i.e., it is only 2.3 kcal/mol higher than the barrier for the sole R_{15} rotation. The concerted $R_{13} + R_{15}$ isomerization reaction implies a much smaller motion of the terminal
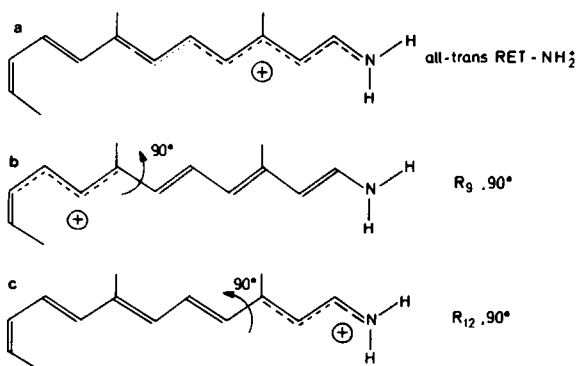

FIGURE 10 π-bonding patterns for RET-NH_2^+ from MNDOC (*a*) in the all-*trans* conformation, (*b*) at the 90° transition state for the double-bond rotation R_9 and (*c*) at the 90° transition state for the single-bond rotation R_{12}.

nitrogen relative to the cyclohexene ring than the sole R_{13} rotation. Therefore, we had suggested previously (17) that the thermal all-*trans* → 13-*cis* isomerization observed during dark adaptation of BR_{568} (5) may comprise an all-*trans* → 13,15-di-*cis* reaction. Recently this conjecture has been verified by NMR (6) and resonance Raman (7) experiments. The calculated barrier of 19.5 kcal/mol is only slightly smaller than the observed activation enthalpy of 24 kcal/mol (53). However, the latter value represents only an upper bound to the calculated value, since it pertains to the retinal-protein complex and may contain energetic contributions due to protein conformational changes, and, therefore, such a difference has to be expected.

A concerted thermal isomerization involving the 11-12 and 13-14 double bonds has been observed recently for the retinal chromophore of squid retinochrome (4), a photopigment that shows common characteristics with the BR chromphore in the effects of salt and pH on the absorption spectrum (54). Here, the direct 11-*cis* → all-*trans* isomerization is hindered by large protein conformational contributions, as indicated by a large activation entropy of 189 cal/(deg × mol) and a correspondingly large activation enthalpy of 82.9 kcal/mol. The consecutive 11-*cis* → 13-*cis* and 13-*cis* → all-*trans* isomerizations require only smaller changes in the protein structure, as indicated by the activation entropies of 8.5 cal/(deg × mol) and 12.8 cal/(deg × mol), respectively. Consequently, the activation enthalpy of 27.5 kcal/mol reported for the concerted rotation R_{11} + R_{13} should be mainly due to retinal. Again, our MNDOC-BWEN barrier of 19.7 kcal/mol for R_{11} + R_{13} is of the correct order of magnitude and is only 0.6 kcal/mol larger than the R_{11} barrier (see Table II). Hence, the occurrence of the concerted R_{11} + R_{13} isomerization suggests, that retinal is bound as a protonated Schiff base also to the retinochrome apo-protein. This inference is corroborated, on the one hand, by the observation that retinochrome reconstituted with 9-*cis* retinal does not induce a thermal isomerization to the all-*trans* form (3) and, on the other hand, by our prediction that the 9-10 double bond is much less affected by protonation than the 11-12 and the 13-14 bonds (see Table II).

In contrast to the concerted double-bond isomerization barriers discussed above, the R_{13} + R_{14} activation energy of 35.2 kcal/mol for the combined isomerization of neighboring single and double bonds is 11 kcal/mol larger than the sum of the activation energies for R_{13} and R_{14} isomerizations. Consequently, if the primary photophysical event in the BR pump cycle involves a simultaneous R_{13} + R_{14} isomerization reaction as we suggest (17, 51, 55), then the thermal reisomerization back to all-*trans* has to proceed by consecutive R_{13} and R_{14} isomerizations. Furthermore, due to the very large R_{14} barrier in the protonated state, only a transient deprotonation allows the R_{14} back reaction to proceed within the millisecond time scale of the cycle explaining, therefore, the occurrence of an unprotonated

intermediate in the pump cycle of BR (51). The high barrier of the R_{13} + R_{14} isomerization provides an explanation how the K intermediate can store 16 kcal/mol energy (3). Such storage requires an energy barrier for the thermal back reaction considerably larger than 16 kcal/mol, i.e., a barrier larger than the 11.5 kcal/mol calculated for R_{13}. Therefore a 13-*cis* K-intermediate should react directly back to BR unless a strong sterical protein-chromophore interaction intervenes. Such a mechanism for the energy storage is feasible, in particular on the short time scale of the lifetime of K or at low temperatures. However it appears more plausible that the converted energy is stabilized by intramolecular forces of the chromophore in a 13,14s-di-*cis* conformation. A 13,14s-di-*cis* geometry is also supported by the result of references 17 and 51 that an all-*trans* → 13,14s-di-*cis* photoisomerization is energetically allowed.

INFLUENCE OF ANIONS ON THE 13-14 ISOMERIZATION BARRIER

The magnitude of the rotation-induced charge shifts in the polyene moiety implies that a protein can selectively steer the stereochemical properties of a $RSBH^+$ by providing an appropriate charge environment. For instance, negative charges in the vicinity of the ring part of the chromophore stabilize the transition states of double-bond rotation and lower the corresponding ground-state isomerization barriers (19, 20) whereas the opposite is true for anions closer to the terminal part. The extent to which a particular torsional barrier is altered depends on the specific location and chemical nature of the charges. Since the distribution and chemical nature of the charges and polar groups around retinal in the binding site of BR are unknown we study here to which degree the isomerization barriers can be changed by a systematic placement of surrounding anions. Thereby we use F^- ions as model anions for computational simplicity.

As discussed in the section entitled Models for the Protein-Chromophore Interaction in BR, for BR the available experimental evidence points towards the existence of a counterion close to the protonated Schiff base of retinal and of a second anion in the vicinity of the polyene chain. Consequently it seems that the pure RSB cations studied so far do not form sufficiently good approximations to the chromophore structure in BR.

The extent to which protonation perturbs the π-system depends on the distance D of the anion from the proton at the Schiff-base nitrogen. A close counterion repulses the π-electrons which, therefore, are not displaced towards the proton. An increased distance D of the counterion implies an increasing displacement of the π-electrons in this direction together with the ensuing bathochromic shift and changes in the bond structure. In fact, an increasing red-shift of the absorption maximum has been shown experimentally on the basis of in vitro measurements using

counterions of increasing size corresponding to larger effective D values (16, 56). The observed spectral shifts are reproduced by simple π-electron calculations assuming different distances of a counterion (22, 23, 24). For the perturbation of the π-system in the ground state the all-*trans* → 13-*cis* activation energy can serve as a measure because this 13–14 double bond is the bond most affected by protonation. We have also chosen this isomerization reaction as a test case because it is known to occur in the dark phase of the BR pump cycle. Similar calculations for R_{11} have strengthened the conclusions drawn below (Tavan, P., and K. Schulten, unpublished results).

Table V A shows the R_{13} activation energies for various distances D of an F^- counterion from the proton at the nitrogen. To avoid the effects of an H^+–F^- charge separation in these calculations, the F^- ion has been kept in a fixed position on the line through the nitrogen and the *trans* proton of the NH_2^+ group during the isomerization. For the smallest distance, $D = 1.5$ Å, the MNDOC-BWEN barrier height of 46.0 kcal/mol is nearly identical to the 46.8 kcal/mol activation energy of the unprotonated compound (see Table I) and the corresponding 13–14 bond is approximately an ordinary π-double bond. Hence, it appears that a close F^- repels the π-electrons strongly

enough to prevent a positive charge from delocalizing into the polyene π-system. Increasing the distance of the anion successively reduces the coulomb repulsion and, at a distance $D = 3.3$ Å, lowers the activation energy to 19.6 kcal/mol. For an infinite separation of the counterion corresponding to the pure cation the barrier is 11.5 kcal/mol. These calculations show that the ground state torsional stability of the 13–14 double bond as well as that of the other π-bonds in the terminal region can be regulated by variation of D. Since in our calculations the distance D represents a measure of the strength of the coulomb attraction between the counterion and the positive charge at the Schiff base, a similar regulation of the $RSBH^+$ structure can be achieved by a protein upon variation of the dielectric shielding of the anion. Neutralization of the counterion produces a chromophore structure similar to that of the pure cation. Spectroscopically this should show up in a strong red-shift of the absorption spectrum as has been observed, indeed, at low pH (25).

If instead of placing an anion into the terminal region (see the section entitled Effect of Protonation on Isomerization Barriers) a protein places the anion towards the ring part of the polyene chain, then the activation energy will be reduced below the pure cation value of 11.5 kcal/mol. This is due to the fact that the anion stabilizes the rotation-induced migration of positive charge to the ring and thereby favors the reversal of the alternating bond structure in the terminal part (see Fig. 10). As an illustration we have calculated the MNDOC R_{13} potential curves for RET—NH_2^+ as a function of the position P_i, where $i = 9$, 11, 13, of the F^- ion. P_i denotes the position above the carbon atom C_i in the plane parallel to that of the polyene at a distance of 3 Å between the planes, i.e., at P_i the anion is located 3 Å "above" C_i. From the data in Table V B it is seen that the R_{13} isomerization barrier becomes smaller when the ion is shifted towards the cyclohexene moiety of the $RSBH^+$. At P_{13} the barrier measures 8.9 kcal/mol, at P_9 the 13–14 bond has become as weak as the 14–15 single bond of the unprotonated molecule (see Table I). Such a scenario with a single counterion in the initial region of the chain probably does not apply to the binding site of retinal in BR because it would imply a reduced perturbation of the π-system upon protonation of the ion and, correspondingly, a blue-shift of the BR absorption at low pH contrary to the experimental findings.

In summary, we may state that a counterion placed at the terminal part of the chain diminishes the effects of protonation on torsional barriers, whereas protonation effects are enhanced if the ion is positioned towards the cyclohexene ring. Of course, these two opposite effects can be combined if two negative ions are positioned around an $RSBH^+$. This is demonstrated by the R_{13} activation energies displayed in Tables VI and VII.

Table VI shows the 13–14 isomerization barriers in case of a close ($D = 1.5$ Å) and a distant ($D = 3.0$ Å) F^- counterion in the terminal region of RET—NEH_2^+ for

TABLE V
R_{13} BARRIERS OF RET – NH_2^+ WITH ONE F^-
COUNTERION

A.

D	SCF		BWEN	
	E_a^*	$E_{(t-c)}\ddagger$	E_a^*	$E_{(t-c)}\ddagger$
	kcal/mol		*kcal/mol*	
1.5	45.8	0.1	46.0	0.5
2.0	35.1	0.4	35.8	0.5
3.0	25.2	0.7	21.6	0.8
3.3	23.4	0.7	19.6	0.4

B.

P_i	SCF		BWEN	
	E_a^*	$E_{(t-c)}\ddagger$	E_a^*	$E_{(t-c)}\ddagger$
	kcal/mol		*kcal/mol*	
P_{13}	11.4	0.1	8.9	0.8
P_{11}	5.2	1.6	4.0	1.4
P_9	1.8	1.2	−0.9	1.0

F^- in the terminal region (A): MNDOC torsional barriers E_a and relative energies $E_{(t-c)}$ of *cis* and *trans* isomers for the rotations R_{13} around the 13–14 bond of the protonated model retinal Schiff-base RET – NH_2^+ as a function of the distance D between the F^- and the proton at the nitrogen. During the torsion the F^- is kept at a fixed distance D from the terminal *trans* hydrogen. F^- in the initial region B: MNDOC torsional barriers for the rotation R_{13} around the 13–14 bond of the protonated model retinal Schiff-base RET – NH_2^+ as a function of the position P_i, where $i = 9, 11, 13$, of the counterion F^- located 3.0 Å above C-atom C_i.
*The energy E_a of the conformation twisted by 90° is defined relative to the lower of the two isomers.
$\ddagger E$(*trans*) − E(*cis*).

TABLE VI

R_{13} BARRIERS OF PROTONATED RET – NH_2^+ WITH TWO F^- IONS

D§	P_i	E_a^*§	$E_{(t-c)}\ddagger$§
1.5	P_{13}	37.2	0.0
	P_{11}	29.0	-0.7
	P_9	25.9	-1.3
3.0	P_{13}	18.7	0.1
	P_{11}	10.6	-1.0
	P_9	6.3	-1.0

MNDOC-BWEN torsional barriers E_a and relative energies $E_{(t-c)}$ of *cis* and *trans* isomers for the rotation R_{13} around the 13–14 bond of the protonated model retinal Schiff-base RET – NH_2^+ as a function of the distance D between the counterion F^- and the proton at the nitrogen and of the position P_i, where i = 9, 11, 13, of a second F^- located 3.0 Å above C-atom C_i.

*The energy E_a of the conformation twisted by 90° is defined relative to the lower of the two isomers.

‡$E(trans) - E(cis)$.

§Energies are given in kilocalories per mole and distances are given in angstroms.

various positions P_i, where i = 9, 11, 13, of a second F^-. In the 1.5 Å case, addition of the second F^- at P_{13} lowers the activation energy from 46.0 kcal/mol to 37.2 kcal/mol. Shifting the second F^- to P_9 yields a reduction to 25.9 kcal/mol. In the 3.0 Å case the dependence of the activation energy on the position of the second ion is analogous, though the activation energy values are much smaller. With the second F^- at P_{11} the barrier (10.6 kcal/mol) is roughly as high as in the case of the pure cation (11.5 kcal/mol), whereas at P_9 with a value of 6.3 kcal/mol it is only half as large. Thus, in the latter case, by the joint action of protonation and of two distant anions, the torsional stability of the 13–14 double bond has been reduced to an order of magnitude characteristic for single bonds in unperturbed polyenes. To investigate the degree of bond order reversal in the terminal part of a RSBH$^+$ for such a charge distribution we have also calculated the isomerization barrier for the neighboring 14–15 single bond. The activation energy of 14 kcal/mol resulting from a MNDOC-BWEN treatment demonstrates that the torsional stability of this single bond has been considerably increased.

The overall reduction of double-bond torsional barriers caused by the positioning of the second negative charge away from the terminal nitrogen is modified by a local effect due to the strong alteration of positive and negative partial charges at the C atoms of the chain in the transition state (see the section entitled Effect of Protonation on Isomerization Barriers). This effect is exhibited in Table VII showing the R_{13} barriers of PL-RET—NH_2^+ with an F^- at the Schiff base in a distance D = 3.0 Å and a second F^- in the initial region of the conjugated system. The double bond of the cyclohexene ring is fully conjugated with the π-system of the chain in this molecule. The

torsional barrier for R_{13} is lowest (5.8 kcal/mol) for the F^- positioned at P_5 above the cyclohexene moiety. Moving the ion along the chain towards the terminal nitrogen leads to a monotonic growth of the R_{13} barrier as long as only positions above odd numbered C-atoms (which acquire positive charge in the transition state) are taken. However, if the ion is also moved above the even numbered C's (which acquire negative charge in the transition state) a small oscillation of the activation energy values E_a is superimposed. For instance, E_a is 3.4 kcal/mol larger at P_{10} than at P_{11}. Again we note that the P_{11} value of E_a (11.4 kcal/mol) is similar to that of the pure cation (11.5 kcal/mol), which shows that the cation can be considered as a good model of the chromophore structure even if two external charges are present in the retinal binding site of BR.

An anion above C_5 induces not only a particularly large weakening of the 13–14 bond but also a reversal of the whole bonding pattern along the chain as indicated schematically in Fig. 11. Hence, one can expect the planarizing force of the 6–7 π-bond to increase strongly enough to overcome the steric hindrances responsible for the 62° dihedral angle between ring and chain in retinal. Though MNDOC is not the most appropriate method to clarify this question, as it exaggerates the torsional effects of steric hindrances for weak π-bonds, the data in Table VIII on the R_6 rotational potential curve still allow very clear conclusions. MNDOC predicts for the cation RETINAL—NH_2^+ a ring-chain conformation twisted by 83° and a planarization barrier of 10.8 kcal/mol. This is probably an overestimate as indicated by the MNDOC/T result, yielding only 6.6 kcal/mol for the barrier. When an F^- is placed 3 Å above C_5 the equilibrium angle as calculated by MNDOC is only 30° and the planarization barrier is reduced to 0.4 kcal/mol. The conformation twisted by 83°

TABLE VII

R_{13} BARRIERS OF PROTONATED PL-RET – NH_2^+ WITH TWO F^- IONS

P_i	E_a^*	$E_{(t-c)}\ddagger$
P_{13}	19.3	0.3
P_{12}	22.8	-0.6
P_{11}	11.4	-0.7
P_{10}	14.8	-1.4
P_9	7.5	-1.0
P_7	6.9	-0.5
P_5	5.8	-1.4

MNDOC-BWEN torsional barriers E_a and relative energies $E_{(t-c)}$ of *cis* and *trans* isomers for the rotation R_{13} around the 13–14 bond of the protonated model retinal Schiff-base PL-RET – NH_2^+ having a first counterion F^- at a distance D = 3.0 Å from the proton at the Schiff-base nitrogen as a function of the position P_i, where i = 5, . . . , 13, of the second F^- located 3.0 Å above C-atom C_i.

*The energy E_a of the conformation twisted by 90° is defined relative to the lower of the two isomers.

‡$E_{(t-c)}$ is $E(trans) - E(cis)$.

§Energies are given in kilocalories per mole.

TABLE VIII
6-7 PLANARIZATION BARRIER OF PROTONATED RETINAL

Case	MNDOC-BWEN			
	$E(0°)$	$E(30°)$	$E(60°)$	$E(83°)$
1	0.0	-3.8	-8.0	-10.8
2	0.0	-.4	1.7	5.4
	MNDOC/T-BWEN			
1	0.0	-2.3	-5.7	-6.6

MNDOC and MNDOC/T torsional potential curves $E(\alpha)$ for the rotation R_6 around the 6-7 bond of protonated retinal. The reaction coordinate α is the dihedral angle between ring and chain. Case 1 refers to RETINAL $-$ NH$_2^+$ without counterion, whereas in case 2 an F$^-$ has been placed 3.0 Å above C_5, i.e., above the cyclohexene ring. Energies are given in kilocalories per mole.

has been lifted strongly by 16.6 kcal/mol showing that the 6-7 bond gains considerable double-bond character. Hence, one can expect that a negative charge near the cyclohexene ring can induce a ring-chain planarization.

The bonding pattern shown in Fig. 11 implies a covalent bond between the terminal nitrogen and the proton and suggests that the protonated state can be stabilized not only by a counterion at the protonated nitrogen but also by an anion above the polyene chain. We have confirmed this hypothesis that a distant anion can shift the pK value of the Schiff-base nitrogen by calculating the energies of RET—NH and RET—NH$_2^+$ in the presence of an anion 3 and 4 Å above C_9, respectively. For the unprotonated compound the state with the anion at a 4 Å distance is 1.0 kcal/mol below the state with the anion at a 3 Å distance. For the protonated molecule the 4 Å state is 7.5 kcal/mol above the 3 Å state. Thus, protonation of the compound is energetically favored by 8.5 kcal/mol if the anion is placed at a distance of 3 Å rather than at a distance of 4 Å. This stabilization corresponds to an increase of the pK by about 6.5 units and can, therefore, rationalize the unusually high pK of 13.3 of the RSB in BR (31).

CHARGE SEPARATION CONTRIBUTION TO ISOMERIZATION BARRIERS

We have demonstrated above how a protein like BR can change the RSB structure of alternating single and double bonds completely by protonation and by placing two or
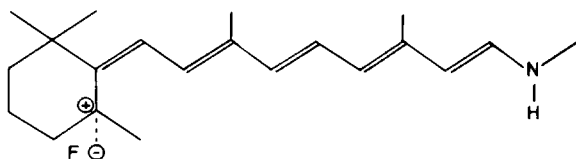

FIGURE 11 Schematic π-bonding pattern for RETINAL-NH$^+$CH$_3$ with an F$^-$ ion above C_5.

more anions into the neighborhood of the chromophore. For the ground state all-*trans* → 13-*cis* isomerization, in particular, activation energies ranging from 6 kcal/mol to 46 kcal/mol, have been calculated depending on the protein-chromophore electrical interactions. The question we will address now is to which extent charge separation in a protein dielectric environment will contribute to these activation energies. This question is motivated by the following consideration: According to our results the unprotonated 13-*cis* RSB of the M$_{410}$ intermediate has to become reprotonated before the isomerization reaction can occur thermally. The reprotonation leaves a negatively charged amino acid side group near the Schiff base that remains at its position while the protonated nitrogen moves away in the course of the 13-14 bond rotation. The resulting separation combined with the dielectric screening of the charges by the protein can explain the extreme red-shift to 640 nm of the reaction product O.

A separation of the counterion from the protonated nitrogen measured by the distance D will have two opposite effects on the barrier height. On the one hand the barrier will decrease since the π-bonding forces decrease with increasing distance D as shown above. On the other hand the barrier will increase due to the coulomb potential between the two charges being separated. To obtain an estimate of the relative importance of these effects we have investigated the 13-14 isomerization reaction for the model RSBH$^+$ RET—NH$_2^+$ in the electric field of a negative charge that is spatially fixed during bond rotation.

If in the all-*trans* conformation an F$^-$ counterion is located at a distance D of 2.8 Å from the *trans* proton of the terminal NH$_2^+$ group and if it is kept fixed at this position, the proton is moved to a distance of 5.3 Å from the F$^-$ ion in the 13-*cis* conformation. As a consequence of this charge separation we predict an energy of the 13-*cis* state $E(0°) = 12.9$ kcal/mole[1] above the all-*trans* state (see Table IX, column 4, for the R$_{13}$ SCF-energy E as a function of the reaction coordinate α). In case that the counterion moves along with the protonated nitrogen at a distance 3 Å the 13-*cis* energy is $E''(0°) = -0.7$ kcal/mol. If no counterion is present the energy is $E'(0°) = -0.5$ kcal/mol (see Tables II and VA and Table IX, columns 6 and 7). Because the barrier height $E(90°) = 31.8$ kcal/mol for a fixed charge is considerably larger than the value $E''(90°) = 24.5$ kcal/mol obtained for the case in which the ion is moving with the terminal group, one might conclude that the charge separation contribution to the barrier greatly exceeds the weakening of the π-bonding forces due to the increasing counterion distance. Furthermore, a thermal all-*trans* → 13-*cis* isomerization reaction might appear to be impossible for a charge distribution like the

[1]All energies are defined relative to the all-*trans* state in this section.

TABLE IX

R$_{13}$ POTENTIAL CURVE WITH ONE SPATIALLY FIXED F$^-$ ION

α*	E_C‡	E_C/ϵ§	E‖	E_I¶	E'**	E''‡‡
180°	0.00	0.00	0.00	0.00	0.00	0.00
120°	20.50	9.79	14.61	4.82	7.80	16.42
90°	43.75	20.88	31.77	10.89	10.66	24.46
60°	36.08	17.22	26.08	8.86	7.62	15.63
0°	28.08	13.40	12.87	−0.53	−0.53	−0.71

Separation of the contributions caused by charge separation and by π-bonding forces to the potential curve for the all-*trans* → 13-*cis* isomerization reaction in the electric field of an F$^-$ counterion spatially fixed with respect to the initial part of RET − NH$_2^+$. Energies are given in kilocalories per mole.

*α is the reaction coordinate; all-*trans* is at 180°, 13-*cis* at 0°.

‡E_C is the coulomb energy of RET − NH$_2^+$ partial charges calculated from MNDOC-SCF in the field of the F$^-$.

§E_C/ϵ is the coulomb energy for dielectric constant ϵ = 2.09.

‖E is the R$_{13}$ MNDOC-SCF potential curve in the electric field of an F$^-$ counterion fixed with respect to the initial part of the molecule.

¶E_I is the contribution of π-bonding forces to E.

**E' is the MNDOC-SCF torsional potential without counterion.

‡‡E'' is the MNDOC-SCF torsional potential with counterion moved along with the terminal region of the molecule.

one considered here because of the very large activation energies $E(90°)$ and $E''(90°)$. However the quantumchemical calculation neglects the dielectric shielding in a protein and, therefore, the potential curves E and E'', treating the case of an unshielded charge in the terminal region of a RSBH$^+$, represent only upper bounds to the torsional potential in a protein environment. Analogously, the E' curve is a lower bound as it refers to the case of a totally shielded counterion.

To obtain an estimate of the potential curve in the dielectric environment of a protein we will determine in an approximate manner the contribution of the charge separation to the torsional potential curve $E(\alpha)$. For this purpose we evaluate at each point of the potential curve the coulomb energy of the molecule in the electric field of the ion by summation over the coulomb energies of the atomic partial charges obtained from the quantumchemical calculation. The resulting coulomb energy E_C shown in Table IX is much too high because the dielectric properties of the RET-NH$_2^+$ molecule have been neglected in this calculation. The magnitude of the error introduced can be estimated by the following comparison: According to the quantumchemical calculations the energy $E(0°)$ is only 12.9 kcal/mol above all-*trans* in the presence of the counterion and −0.5 kcal/mol below all-*trans* in its absence as follows from the $E'(0°)$ value in Table IX. The resulting increase $\Delta E(0°)$ of the *cis* state energy due to the action of the counterion is $\Delta E(0°) = E(0°) − E'(0°) =$ 13.4 kcal/mol. This energy is smaller, however, than the coulomb energy difference between the *cis* and the all-*trans* state, which measures 28.1 kcal/mol. The difference

can be attributed to a dielectric shielding effect arising from the electrons in RET-NH$_2^+$, which is accounted for in the quantumchemical calculation. The corresponding dielectric constant is: $\epsilon = E_C(0°)/\Delta E(0°) = 2.1$. In the 13-*cis* conformation the molecule has the largest average distance from the ion compared to all the other points on the reaction path. Therefore, the shielding of the charge by the molecule is better for points close to the all-*trans* conformation and the dielectric shielding will be more effective for these points. Also, in a protein environment one can expect an additional contribution to the dielectric constant due to the protein environment.

Considering ϵ as an average constant along the reaction path and scaling the coulomb energies $E_C(\alpha)$ with ϵ as determined above one obtains an approximation and upper bound for the coulomb contribution to the potential curve $E(\alpha)$. Subtracting the scaled coulomb contribution E_C/ϵ from E gives an estimate and lower bound for the contribution $E_I(\alpha)$ of the internal forces to $E(\alpha)$ through: $E_I(\alpha) = E(\alpha) − E_C(\alpha)/\epsilon$. E_C/ϵ and E_I are given in columns 3 and 5 of Table IX, respectively. If the charge distribution around retinal in the binding site of bacteriorhodopsin was as given and if steric interactions between the protein and retinal could be neglected, then one could construct from E_C and E_I a realistic potential curve by adding to the internal contribution E_I a coulomb contribution E_C/ϵ' scaled with a dielectric constant $\epsilon' > \epsilon$ that accounts for additional shielding effects due to the protein.

We will now discuss the effect of the protein dielectric constant ϵ'. The value of ϵ' is unknown but it determines sensitively the properties of the potential curve. The choice $\epsilon' = 5$, for instance, gives an activation energy $E_a = 19.6$ kcal/mol. This barrier is lower than the E'' value of 24.5 kcal/mol showing that in a protein environment the decrease of bond stability upon removal and dielectric shielding of the counterion can overcompensate its increase due to the corresponding charge separation. Also, the calculated barrier is low enough to allow a thermal isomerization to proceed within a few seconds. If one applies this estimate to determine the coulomb energy stored in an all-*trans* → 13-*cis* photoisomerization one arrives at a value of 5 kcal/mol. This low energy value limits the extent to which the primary form of energy stored in the light-driven pump cycle of BR can be a coulomb energy derived from charge separation upon 13-*cis* isomerization, as suggested in reference 27, if the choice $\epsilon' = 5$ is realistic. An even larger choice of $\epsilon' = 15$ for the dielectric constant inside a protein yields an R$_{13}$ barrier of 13.8 kcal/mol that is similar to that of the pure cation and corresponds to a time scale of milliseconds for thermal isomerization. Hence, if one assumes a rather strong shielding of electrical charges by a protein environment, then it appears that the sterochemical properties of the RSBH$^+$ in BR might be rather well represented by the pure cation investigated in the section entitled Effect of Protonation on

TABLE X
R_{13} POTENTIAL CURVE WITH TWO SPATIALLY FIXED F^- ION

α	E_C	E_C/ϵ	E	E_1	E'	E''
180°	0.00	0.00	0.00	0.00	0.00	0.00
120°	20.75	11.79	12.31	0.52	0.29	6.04
90°	25.99	14.77	15.66	0.90	0.69	8.30
60°	24.40	13.86	14.08	0.22	0.03	6.25
0°	16.73	9.50	8.35	−1.16	−1.16	1.01

See the caption to Table IX. For this calculation a second F^- ion has been added 3 Å above C_9 and for the dielectric constant ϵ a value of 1.76 has been calculated.

Isomerization Barriers. This result justifies a posteriori that we have taken the data on the cation as a reference for comparisons with observations on BR.

To test the validity of the concept of an average dielectric constant we compare in Table IX the internal contribution $E_1(\alpha)$ with the potential curve $E''(\alpha)$ for the protonated RET—NH$_2^+$ without counterion. As we have stated above, the latter curve represents a lower bound to the torsional barrier of the 13–14 bond in case a counterion is attached to the RSBH$^+$. For the transition state at 90° and for the 60° conformation, for which the average distance between the ion and the molecule is comparable to the 13-*cis* conformation, the E_1 values are only slightly larger than the corresponding E' values. This indicates, that the influence of the ion on the binding forces of the molecule is rather weak in these configurations. The low value of E_1 at 120° shows that we underestimated, as expected, the dielectric shielding for conformations close to all-*trans*.

All these inferences are corroborated by a similar analysis of the data in Table X referring to a charge distribution, in which an additional F^- ion has been put on position P_9. The upper bound to the barrier in this case if 15.7 kcal/mol, the lower bound is 0.9 kcal/mol, and with $\epsilon' = 5$ one derives an activation energy of 6.1 kcal/mol which, again, is smaller than the value $E''(90°) = 8.3$ kcal/mol calculated for the counterion moving with the terminal group. Due to the second ion in the initial region all barriers are greatly reduced and allow thermal isomerizations to proceed at rates ranging from $\sim 10^3$ to 10^9s^{-1} and larger. Hence, one can expect that for both charge distributions an isomerization around the 13–14 bond can become thermally feasible in a protein environment even if the coulomb attraction to a spatially fixed counterion is taken into account.

SUMMARY

It has been well known for a long time that protonation and electrical interactions induce strong shifts of the spectrum of retinal, an effect which has been invoked to explain the different absorption maxima of the visual pigments and of bacteriorhodopsin. This explanation extends to the inter-mediates appearing after optical excitation of the rhodopsins and of bacteriorhodopsin, e.g., to the sequences prelumi-, lumi-, m_I-, m_{II}-rhodopsin and K-, L-, M-, N-, and O-bacteriorhodopsin. In this article we have provided evidence that the chromophore-protein interactions reflected by the spectral differences of these intermediates deserve particular attention. On the basis of quantum-chemical calculations we have demonstrated that the same interactions that induce spectral shifts of the retinal chromophore do also alter its ground state stereochemical properties in very specific ways. Protonation and deprotonation of the retinal Schiff base together with electrical interactions can steer the chromophore along a desired stereochemical pathway. We found that protonation of the Schiff-base nitrogen alters the isomerization barriers of retinal in that double-bond rotational barriers are lowered, e.g., from 47 kcal/mol to 11.5 kcal/mol for the 13–14 bond, and single-bond isomerization barriers are increased, e.g., to values up to 20 kcal/mol for the 14–15 bond. Thus protonation makes double-bond isomerizations thermally feasible on the time scale of a millisecond, whereas thermal single-bond isomerizations can be prevented on that time scale. Protonation can also make those isomerization processes thermally feasible that involve simultaneously two double bonds. For example, the barrier for an all-*trans* → 11,13-di-*cis* (13,15-di-*cis*) isomerization is predicted at 19.7 (19.5) kcal/mol.

Electrical interactions with negative ions also contribute to the magnitude of isomerization barriers. Negative ions near the protonated Schiff-base nitrogen shift barriers in the direction of their conventional polyene values, whereas negative ions near the cyclohexene ring have the reverse effect. Positioning, for instance, a negative F^- ion 3 Å near the proton at the Schiff-base nitrogen produces an all-*trans* → 13-*cis* barrier of 25.2 kcal/mol, adding a second ion 3 Å above C_9 lowers the barrier to 6 kcal/mol. These barriers heights result when the first F^- ion rotates along with the isomerizing retinal at a fixed juxtaposition to the Schiff-base nitrogen. However, our calculations have demonstrated that in a protein environment thermal double-bond isomerizations can also be reconciled with a spatially fixed counterion. Negative ions near the cyclohexene ring have the additional effects of bringing the pK of the Schiff-base nitrogen to values above 10 units and to introduce a ring-chain planarization.

Our computational results indicate that the bathochromic shifts of protonated retinal Schiff bases are accompanied by profound alterations of the ground-state stereochemical properties. The stereochemical properties predicted appear significant in view of retinal's role during the activity of squid retinochrome, rhodopsin, and bacteriorhodopsin and support the suggestion in references 17, 51, and 55 that the stereochemical pathway of retinal during the pump cycle of bacteriorhodopsin involves the sequence of stereoisomers all-*trans*, 13,14s-di-*cis*, (deprotonation), 13-*cis*, (protonation), all-*trans*.

REFERENCES

1. Stoeckenius, W., and R. Bogomolni. 1982. Bacteriorhodopsin and the purple membrane of halobacteria. *Annu. Rev. Biochem.* 51:587.

2. Stoeckenius, W., R. H. Lozier, and R. Bogomolni. 1979. Bacteriorhodopsin and related pigments of halobacteria. *Biochim. Biophys. Acta.* 505:215.

3. Birge, R. and T. M. Cooper. 1983. Energy storage in the primary step of the photocycle of bacteriorhodopsin. *Biophys. J.* 42:61–69.

4. Ozaki, K., R. Hara, T. Hara, and T. Kakitani. 1983. Squid retinochrome: configurational changes of the retinal chromophore. *Biophys. J.* 44:127–137.

5. Maeda, A., T. Iwasawa, and T. Yoshizawa. Isomeric composition of retinal chromophore in dark-adapted bacteriorhodopsin. *J. Biochem.* 82:1599.

6. Harbison, G. S., S. O. Smith, J. A. Pardoen, C. Winkel, J. Lugtenburg, J. Herzfeld, R. Mathies, and R. G. Griffin. 1984. Dark-adapted bacteriorhodopsin contains 13-cis, 15-syn and all-trans, 15-anti retinal Schiff bases, *Proc. Natl. Acad. Sci. USA.* 81:1706.

7. Smith, S. O., A. B. Myers, J. A. Pardoen, C. Winkel, P. P. J. Mulder, J. Lugtenburg, and R. Mathies. 1984. Determination of retinal Schiff base configuration in bacteriorhodopsin, *Proc. Natl. Acad. Sci. USA.* 81: 2055.

8. Hudson, B. S., B. E. Kohler, and K. Schulten. 1982. Linear polyene electronic structure and potential surfaces. *Excited States.* 6:1.

9. Ackermann, J. R., and B. E. Kohler. S-cis octateraene: ground state barrier for s-cis to s-trans isomerization. *J. Chem. Phys.* In press.

10. Honig, B., U. Dinur, K. Nakanishi, V. Balogh-Nair, M. A. Gawinowicz, M. Arnaboldi, and M. Motto. 1979. An external point-charge model for wavelength regulation in visual pigments. *J. Am. Chem. Soc.* 101:7084.

11. Erickson, J. O., and P. E. Blatz. 1968. N-Retinylidene-1-amino-2-propanol: a Schiff base analog for rhodopsin. *Vision Res.* 8:1367.

12. Autrum, H., and V. von Zwehl. 1964. Die spektrale Empfindlichkeit einzelner Sehzellen des Bienenauges, *Z. Vergl. Physiol.* 48:357.

13. Bernard, G. D. Red-absorbing visual pigment of butterflies. 1979. *Science (Wash. DC).* 203:1125.

14. Schulten, K., U. Dinur, and B. Honig. 1980. The spectra of carbonium ions, cyanine dyes, and protonated Schiff base polyenes. *J. Chem. Phys.* 73:3927.

15. Sorensen, T. S. 1965. The preparation and reactions of a homologous series of aliphatic polyenylic cations. *J. Am. Chem. Soc.* 87:5075.

16. Irving, C. S., G. W. Byers, and P. A. Leermakers. 1970. Spectroscopic model for the visual pigments. Influence of microenvironmental polarizability. *Biochemistry.* 9:858.

17. Orlandi, G. and K. Schulten. 1980. Coupling of stereochemistry and proton donor-acceptor properties of a polyene Schiff base. A model of a light-driven proton pump. *Chem. Phys. Lett.* 64:370.

18. Thiel, W. 1981. The MNDOC Method, a Correlated Version of the MNDO Model. *J. Am. Chem. Soc.* 103:1413.

19. Warshel, A., and C. Deakyne. 1978. Coupling of charge stabilization, torsion and bond alternation in light-induced reactions of visual pigments. *Chem. Phys. Lett.* 55:3.

20. Warshel, A. Conversion of light energy to electrostatic energy in the proton pump of *Halobacterium Halobium.* 1979. *Photochem. Photobiol.* 30:285.

21. Kropf, A., and R. Hubbard. 1958. The mechanism of bleaching rhodopsin. *Ann. NY. Acad. Sci.* 74:266.

22. Suzuki, H., T. Komatsu, and T. Kato. 1973. Theory of the optical property of retinal in visual pigments. *J. Phys. Soc. Jpn.* 34:156.

23. Suzuki, H., T. Komatsu, and H. Kitajima. 1974. Theory of the optical property of visual pigment. *J. Phys. Soc. Jpn.* 37:177.

24. Honig, B., A. Greenberg, U. Dinur, and T. G. Ebrey. 1978. Visual pigment spectra: implications of the protonation of the retinal Schiff base. *Biochemistry.* 15:4593.

25. Fischer, U., and D. Oesterhelt. 1979. Chromophore equilibria in bacteriorhodopsin. *Biophys. J.* 28:211–230.

26. Fischer, U., and D. Oesterhelt. Changes in the protonation state of bacterio-opsin during reconstitution of bacteriorhodopsin. *Biophys. J.* 31:139–146.

27. Honig, B., T. G. Ebrey, R. H. Callender, U. Dinur, and M. Ottolenghi. 1979. Photoisomerization, energy storage, and charge separation: a model for light energy transduction in visual pigments and bacteriorhodopsin. *Proc. Natl. Acad. Sci. USA.* 76:2503.

28. Braiman, M., and R. Mathies. Resonance raman spectra of bacteriorhodopsin's primary photoproduct: evidence for a distorted 13-cis retinal chromophore. 1982. *Proc. Natl. Acad. Sci. USA.* 79:403.

29. Braiman, M., and R. Mathies. 1983. Structural relaxation of the Schiff base bond in bacteriorhodopsin's Primary Photoproduct. *Biophys. J.* 41 (2, Pt. 2): 14a. (Abstr.)

30. Smith, S. O., and R. Mathies, 1983. The structure of the chromophore in the O_{640} intermediate of bacteriorhodopsin. *Biophys. J.* 41 (2, Pt. 2):13a. (Abstr.)

31. Druckmann, S., M. Ottolenghi, A. Pande, J. Pande, and R. H. Callender. 1982. Acid-base equilibrium of the Schiff base in bacteriorhodopsin. *Biochemistry.* 21:4953.

32. Schreckenbach, T., B. Walckhoff, and D. Oesterhelt. 1977. Studies on the retinal-protein interaction in bacteriorhodopsin. *Eur. J. Biochem.* 6:499.

33. Gärtner, W., P. Towner, H. Hopf, and D. Oesterhelt. 1983. Removal of methyl groups from retinal controls the activity of bacteriorhodopsin. *Biochemistry.* 22:2637.

34. Schreckenbach, T., B. Walckhoff, and D. Oesterhelt. Specificity of the retinal binding site of bacteriorhodopsin: chemical and stereochemical requirements for the binding of retinol and retinal. *Biochemistry.* 17:5353.

35. Schreckenbach, T., B. Walckhoff, and D. Oesterhelt. 1978. Properties of the retinal binding site in bacteriorhodopsin: use of retinol and retinyl moieties as fluorescent probes. *Photochem. Photobiol.* 28:205.

36. Nakanishi, K., V. Balogh-Nair, M. Arnoldi, K. Tsujimoto, and B. Honig. 1980. An external point-charge model for bacteriorhodopsin to account for its purple color. *J. Am. Chem. Soc.* 102:7945.

37. Derguini, F., C. G. Caldwell, M. G. Motto, V. Balogh-Nair, and K. Nakanishi. 1983. Bacteriorhodopsins containing cyanine dye chromophores. Support for the external point charge model. *J. Am. Chem. Soc.* 105:646.

38. Kakitani, T., H. Kakitani, B. Honig, and K. Nakanishi. 1983. Symmetric charge distribution in the bacteriorhodopsin binding site. *J. Am. Chem. Soc.* 105:648.

39. Dinur, U., B. Honig, and K. Schulten. 1980. On the nature of excited states in cyanine dyes: Implications for visual pigment spectra. *Chem. Phys. Lett.* 72:493.

40. Dewar, M. J. S., and W. Thiel. 1977. Ground states of molecules. 38. The MNDO method. Approximations and parameters. *J. Am. Chem. Soc.* 99:4899.

41. Epstein, P. S. 1926. The stark effect from the point of view of Schroedinger's quantum theory. *Phys. Rev.* 28:695.

42. Nesbet, R. K. 1955. Configuration interaction in orbital theories. *Proc. R. Soc. Lond. Ser. A.* 230:312.

43. Pople, J. A., and G. A. Segal. Approximate self-consistent molecular

orbital theory. III. CNDO results for AB_2 and AB_3 systems. *J. Chem. Phys.* 44:3289.

44. Bingham, R. C., M. J. S. Dewar, and D. H. J. Lo. 1975. Ground states of molecules. 25. Mindo/3. An improved version of the MINDO semiempirical SCF-MO method. *J. Am. Chem. Soc.* 97:1285.

45. Payne, P. W., and L. C. Allen. 1977. Barriers to Rotation and Inversion. *Modern Theoretical Chemistry.* 4:29.

46. Flanigan, M. C., A. Komornicki, and J. W. McIver, Jr. Ground state potential surfaces and thermochemistry. 1972. *Modern Theoretical Chemistry.* 8:1.

47. Hamanaka, T., T. Mitsui, T. Ashida, and M. Kakudo. 1972. The crystal structure of all-trans-retinal. *Acta Cryst. B.* 28:214.

48. Gieren, A., V. Lamm, D. Oesterhelt, and H. J. Schlude. 1982. Röntgenstrukturanalyse des 4-keto-all-trans-retinals. *Z. Naturforsch.* 37b:1612.

49. Wadell, W. H., A. M. Schaffer, and R. S. Becker. 1977. Visual Pigments. 7. Experimental and theoretical investigations of the absorption spectral properties of protonated retinal Schiff bases and implications for the bathochromic shift in visual pigments. *J. Am. Chem. Soc.* 99:8456.

50. Birge, R. R., and L. M. Hubbard. 1980. Molecular dynamics of cis-trans isomerization in rhodopsin. *J. Am. Chem. Soc.* 102:2195.

51. Schulten, K., Z. Schulten, and P. Tavan. 1984. An isomerization model for the pump cycle of bacteriorhodopsin. In International Conference on Biological Membranes, Information and Energy Transduction in Biological Membranes. 10th. L. Bolis, E. J. M. Helmreich, and H. Passow, editors. Allan R. Liss, Inc., NY. 113–131.

52. Warshel, A. 1976. Bicycle-pedal model for the first step in the vision process. *Nature (Lond.).* 260:679.

53. Tokunaga, F., and T. Ebrey. 1978. The blue membrane: the 3-dehydroretinal-based artificial pigment of the purple membrane. *Biochemistry.* 17:1915.

54. Ozaki, K., R. Hara, and T. Hara. 1982. Dependency of absorption characteristics of retinochrome on pH and salts. *Exp. Eye Res.* 34:499.

55. Schulten, K., and P. Tavan. 1978. A mechanism for the light-driven proton pump of *Halobacterium halobium. Nature (Lond.).* 272:85.

56. Blatz, P. E., and J. H. Mohler. 1975. Effect of selected anions and solvents on the electronic absorption, nuclear magnetic resonance, and infrared spectra of the N-retinylidene-n-butylammonium-cation. *Biochemistry.* 14:2304.